University of Glasgow
DEPARTMENT OF
AEROSPACE
ENGINEERING

A Statistical Analysis Of Surface Pressure Measurements With Particular Reference To Vortex Breakdown.

M. Jupp[1], F. Coton[2] and R. Green[3]

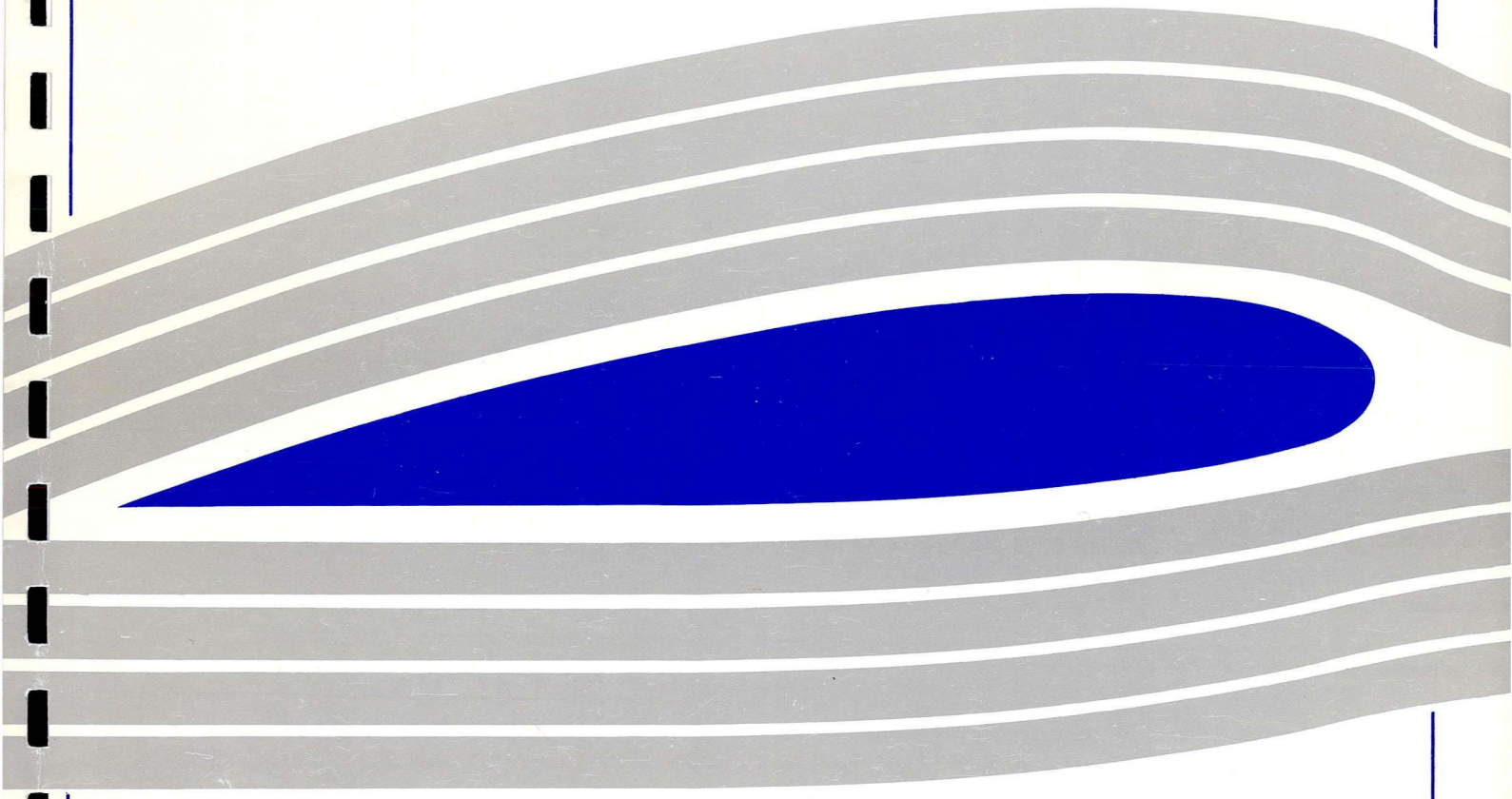

G.U. Aero Report No. 9806

A Statistical Analysis Of Surface Pressure Measurements With Particular Reference To Vortex Breakdown.

M. Jupp[1], F. Coton[2] and R. Green[3]

Department of Aerospace Engineering

James Watt Building South

University of Glasgow

Glasgow G12 8QQ

April 1998

[1] Research Student
[2] Senior Lecturer
[3] Lecturer

SUMMARY

This paper describes and presents results from static wind tunnel tests conducted on a 60° delta wing at a root chord Reynolds number of 2.7 x 10^6. In these tests, the wing was instrumented with 192 miniature pressure transducers which, in conjunction with a powerful multi-channel data-logging system, allowed the distribution of time-varying surface pressures to be measured at high temporal resolution. Analysis indicates that the distribution of root-mean-square pressure on the leeward surface of the wing can provide considerable insight into the behaviour of both the primary and secondary vortex structures. In addition, it has been established that the frequency content of pressure signals measured in the vicinity of these vortex structures is sensitive to the vortex state. It is suggested that these data features can be directly attributed to previously observed behavioural characteristics of the vortex breakdown process.

NOMENCLATURE

c	root chord.
f	frequency, (Hz).
n	non-dimensional frequency parameter, ((fc/U) sin α).
n_m	modified non-dimensional frequency parameter, ((fc cot Λ/U) sin α).
Re	Reynolds number based on root chord.
RMS	root-mean-square.
s	local semi-span.
U	mean freestream velocity.
x	chordwise distance from apex.
x/c	non-dimensional chord position.
y	spanwise distance from wing centreline.
y/s	non-dimensional span position.
0.5 q^2	turbulent kinetic energy.
2s	local span.
α	model incidence.
α_v	helix angle of velocity at the vortex core.
υ	axial component of velocity at the vortex core.
ω	radial component of velocity at the vortex core.

Subscripts

bd	location of breakdown position.
m	modified.
te	trailing edge.

LIST OF CONTENTS

1.0 INTRODUCTION

The behaviour of vortical flows on the leeward surface of sharp-edged delta wings has been the subject of research since the early 1950's. The flow is dominated by a pair of vortical structures, known as the primary vortices, the centrelines of which extend from the wing apex, along a ray located somewhere inboard of each leading-edge and into the wake beyond the trailing-edge of the wing. The location and height above the wing of each centreline is chiefly dependent on angle of attack, the sweep angle and leading-edge profile [1]. The creation of these primary vortices causes the attached boundary layer underneath each structure to turn outboard towards the leading-edge. This outflow meets a spanwise pressure gradient, which is adverse in the direction of the leading-edge, causing the flow to separate into a secondary shear layer. This, in turn, rolls up into a secondary vortex structure rotating in opposition to its primary parent. The main effect of the secondary vortex is to displace the primary vortex upwards and inwards; the effect being greater if the boundary layer is laminar, where separation occurs earlier, increasing the size of the secondary vortex structure.

These vortical structures tend to grow in strength as the wing incidence is increased further and their effect increasingly dominates the total lift curve of the wing. The formation of vortices allows the generation of useable lift to continue at angles of incidence beyond the recognized stall condition of conventional wings. However, at some value of incidence and at some point along the vortex core, a sudden transformation takes place causing the axial velocity of the flow to stagnate and the vortex to break down into large scale turbulence. This phenomenon of vortex 'burst' has greatly interested researchers since it was apparently first observed by Elle in 1960 [2] and defined by Lambourne & Bryer in 1962 [1].

The majority of experimental research programmes in this area has made use of flow-visualisation techniques to clarify the physical mechanisms involved in the formation, maintenance and eventual breakdown of vortical flows. By and large, these investigations have been very successful in identifying the principal features of the flow for wings of various aspect ratio. Similarly, the location of vortex burst over a wide range of fixed angles of attack has been measured on a number of stationary

wings [3,4,5] and the hysteretic nature of vortex burst, together with the gross effects of pitch rate and oscillation frequency, has been observed on a series of pitching and oscillating wings [6,7,8,9,10,11].

A smaller number of research programmes have successfully measured the transient flow-field characteristics of delta wings during pitch-up motions to very large angles of attack. These have used both Velocity Probe measurements [12,13] and non-intrusive techniques such as Laser-Doppler Anemometry (LDA) [14,15,16] and Particle-Image Velocimetry (PIV)[17,18,19]. These measurements have enabled the construction of two-dimensional cross-flow velocity fields, from which the flow features previously observed during flow-visualisation experiments, have been quantified.

In addition to the methods described above, surface pressure measurement has proved to be a valuable tool in the study of delta wing flows. Often, however, limitations of the data acquisition system, or the particular pressure measurement technique applied, have severely limited the detailed information obtained. Indeed, most studies have either used low spatial resolution or have focused on specific sections of the wing [20,21,22]. Very rarely have detailed full-surface pressure data been presented. Where this has been possible [23], results have exhibited a low pressure ridge associated with the leading edge vortex but no distinct response in the local pressure has been detected during vortex breakdown. Rather, it has been proposed that the shape of the spanwise pressure distribution may be sensitive to the vortex state and may, thus, provide a basis for identifying breakdown [24].

Significantly, most of these studies have been limited to the measurement of mean pressure distributions and have, therefore, neglected the potentially valuable information contained in the time-varying signal. Studies involving analysis of surface pressure fluctuations have been primarily targeted at determining post-breakdown buffet characteristics of the wing flow [25,26,27]. In this respect, much valuable information has been forthcoming and has provided useful insight into the buffet phenomenon. In some cases additional information on the evolution and structure of the leading-edge vortex system has also been obtained.

In a study by Gursul [25], on a series of delta wing planforms, it was found that the pressure spectra in the post-breakdown region of the wing exhibited a dominant frequency component which was not present prior to breakdown. It was established that this frequency was associated with the helical mode instability of the vortex breakdown field and that it was possible to use its presence as an indication of the progression of breakdown over the wing.

Analyses of frequency spectra and root-mean-square values of surface pressure fluctuations were also conducted by Woods and Wood [27] on two novel wing planforms. In general, the results obtained were consistent with those of Gursul although an additional higher buffet frequency was identified in the region of vortex attachment on one of the wings. It was also noted there existed a peak in the RMS value of the surface pressure near the attachment line of the vortex. This observation was confirmed in a study by Honkan and Andreopoulos [12] who used a novel transducer arrangement together with off-body measurements to study the vorticity distribution over a delta wing. They also identified a region of high turbulent kinetic energy just outboard of the attachment location but inboard of the primary vortex core. It was also established that the attachment zone itself corresponded to a peak in the local spanwise mean vorticity.

This report presents results from a series of experiments conducted on a sharp-edged 60° delta wing in the Handley-Page wind-tunnel facility at Glasgow University. The upper surface of the delta wing was highly instrumented on one side with miniature pressure transducers. These were connected to a powerful two-hundred channel data acquisition system which has the capability to acquire data at the rate of 50kHz per channel. This allowed surface pressure data to be obtained at high spatial and temporal resolution over a wide range of incidence. A series of low-speed flow visualisation tests were also conducted to provide supplementary qualitative flow field information.

Analysis of the collected data indicates that it is possible, on the basis of surface pressure measurements alone, to monitor the structure and location of the leading edge vortex system. The progression of breakdown towards the apex of the wing with increasing incidence can also be tracked with a high degree of confidence. In fact, it has been shown that key events in the breakdown process may be manifest as discrete changes in the frequency content of individual pressure signals. Once breakdown has been established over the wing, analysis of the frequency spectra yields dominant non-dimensional buffet frequencies which generally compare well to the correlation of Mabey [26].

2.0 EXPERIMENTAL METHOD

Two types of wind tunnel tests took place, namely pressure measurement tests and smoke flow visualisation tests. These tests took place in different facilities, which are described as follows.

2.1 Pressure Measurement Tests

2.1.1 Model Design and Construction

The basic delta wing used in the main test programme was machined from a solid block of aluminium. It had an 800mm root-chord, and a sweep angle of 60°. This gave an aspect ratio of 2.31 and a trailing edge span ($2s_{te}$) of 923.8mm. The wing had a flat leeward surface, a highly contoured windward surface, (giving a thickness ratio of 9.0%) and bevelled edges on the windward side to produce sharp leading and trailing edges. The model was designed to accommodate 192 Kulite Type CJQH-187 differential pressure transducers located primarily on the starboard side of both the leeward and windward surfaces. The shape of the windward surface and the location of the leeward surface transducers is shown in Figure 1.

2.1.2 The Wind-Tunnel Facility

The tests were conducted in the Department's Handley-Page wind-tunnel facility. This is a closed return type wind tunnel with an octagonal test section measuring 2.13m by 1.61m (working area = 2.667m^2), which gave a model-span to tunnel width ratio of 43.4% and a model blockage (not including strut fairings) of 1.25% to 9.27% over the incidence range $0° \leq \alpha \leq 42°$. The model was mounted leeward side up, and was supported by three vertical struts, one placed at the quarter chord position and two at the trailing edge. The forward strut was rigidly fastened to a support structure mounted on a concrete floor below the wind tunnel. The two rear struts were connected to a hydraulic actuation mechanism, which, for static testing, was used to adjust the angle of incidence of the wing to an accuracy of $\pm 0.1°$

2.1.3 The Data Acquisition System

Data acquisition was carried out by a PC equipped with a 486 processor, programmed using TEAM 256 software. The PC was configured and interfaced with propriety Bakker Electronics BE256 modules which provided the necessary analogue to digital conversion. The system had 200 channels, each capable of sampling at 50kHz. The channels not taken up by transducers were used to sample temperature, barometric pressure, reference dynamic pressure and model incidence. The signals from each transducer were delivered to a specially designed signal conditioning unit of modular construction, and each module contained its own control board. The control board was capable of automatic offset and gain adjustment by sampling the minimum and maximum output of each transducer during each run and adjusting the gains automatically as required.

2.1.4 Experimental Procedure

During testing, the wing was set at a starting incidence of -5°. The wing was then pitched up in 1° increments to + 42°. A suitable period was allowed prior to data collection at each incidence and the pressure data were then sampled at a frequency of 2.0kHz for a period of 1s. The total data set was divided into three 'runs' each covering an arc of 16°, giving a data set of 32000 samples per run. The mean free stream velocity was measured at $50ms^{-1}$, which gave a Mach number of 0.16 and a Reynolds number of 2.7×10^6 based on root chord.

2.2 Smoke Flow Visualisation Tests

The model tested in the flow visualisation facility was geometrically similar to the model used for the pressure measurement tests, and had a root chord of 346mm and a trailing edge span of 400mm. The model was also mounted in a similar fashion. In this case, the mechanism for pitching the model was provided by a ball screw and flange nut assembly below the tunnel floor. The two rear support struts were attached to the nut by a yoke, so as the screw shaft rotated the yoke moved in the vertical direction. The contoured shape of the windward surface of the model was used to house a plenum chamber for smoke flow visualisation purposes. Smoke was then ejected from

0.2mm slots machined along the whole leading edge and 2mm below the top surface of the model.

The flow visualisation facility is a non-return type wind tunnel with a square working section of 0.9m x 0.9m, which gave a span to tunnel width ratio of 44.4% and a model blockage of 0.77% to 5.72% over the same incidence range as the pressure measurement tests. All tests which were carried out at a mean free stream speed of $0.44ms^{-1}$ which gave a nominal Reynolds number of 10000 based on root chord. The justification for carrying out these tests at low Reynolds numbers on scaled down models is based on the findings of Atta & Rockwell [6]. They reported that the position of vortex breakdown on a stationary wing did not change significantly over the Reynolds number range $2900 \leq Re \leq 13400$, and agreed well with other investigations up to $Re = 10^6$. Similarly, Lambourne & Bryer [1] showed previously that vortex breakdown position is largely independent of Reynolds number in the range $Re = 10000$ to 4.6×10^6.

Illumination was provided by a Cyonics 0.5W Argon ion laser of 525nm-480nm wavelength located above the wind tunnel. Suitably arranged mirrors expanded the beam into a thin sheet, which shone down into the wind tunnel. The whole system was mounted on a trolley such that movement of the trolley along the length of the wind tunnel and adjustment of the optics allowed the light sheet to be positioned at any chosen chord station or at any lateral angle relative to the trailing edge. The tests were carried out by positioning the laser light sheet parallel to the trailing edge at a chord position (x/c) of 0.95. The model was then placed at a starting incidence of 0° (accurate to within to ± 0.5°), and was then pitched up in increments of 0.5° until breakdown was observed to pass through x/c = 0.95. Then at each higher incidence the light sheet was positioned at the chord location where the vortex core was seen to fluctuate between breakdown and reformation. This chord position was recorded against incidence.

3.0 RESULTS

3.1 Pressure Measurements

For a given transducer, the pressure data at each angle of incidence were non-dimensionalised and averaged to produce values of mean C_P. The uncertainty in the pressure coefficient values obtained in this way is $\pm$ 0.5%. A study of the mean C_P data revealed the growth of a localised 'suction' region on the leeward surface of the wing extending from the apex towards the trailing edge. This suction region first became apparent in the data at an incidence of 2° with a peak in the form of a ridge located along a ray at span station (y/s) = 0.7. Figure 2 shows a series of contour plots indicating the mean C_P distribution on the leeward surface of the wing at various incidences. The plots are indicative of a general trend. That is, for all angles of incidence the magnitude and localisation of the suction peak were at a maximum at the apex of the wing, with a decrease in magnitude and a broadening of the peak towards the trailing edge. Similarly, the suction region increased in magnitude and tended to move inboard as the wing was pitched up. These findings were in keeping with the results presented previously by Parker [28], Jarrah [29] and Thompson et al [30]. Previous work [28] has shown that this region of high negative C_P corresponds more or less to the location above the wing of the centreline of the primary vortex core. For the incidences shown in Figure 2, the vortex is fully developed and the path of the centreline of the vortex core can be clearly seen (1).

The distribution of negative C_P across the span of the wing for four angles of incidence (14°, 16°, 18° and 20°) at two chord stations (x/c = 0.2 and 0.3875) is shown in Figure 3. The increase in peak suction with incidence is clearly seen at x/c = 0.2, although its decrease from 18° to 20° is thought to be significant. Similarly, the inboard shift of the suction peak with incidence, which is apparent at all but the most forward chord stations, is shown at x/c = 0.3875. It is clear from both plots that, like the corresponding contour plots, there is a reduction in magnitude as well as a broadening of the suction region with distance from the apex.

3.2 Analysis Of The Root-Mean-Square Pressure Distribution

In addition to the study of the mean C_P distribution, the root-mean-square (RMS) of the pressure deviations around the mean were examined at each angle of incidence. Figure 4 shows a series of contour plots of the RMS pressure distribution on the leeward surface of the wing at incidences of 3°, 5°, 7° and 9°. Examination of the distribution shows the growth of a region of high RMS pressure in the form of a ridge located along a ray from the apex towards the trailing edge. The initial appearance of this high RMS pressure region occurs at an incidence of 1°. Like the mean C_P distribution, the region of high RMS grows in strength with an increase in incidence, but unlike the mean C_P distribution its strength does not diminish with distance from the wing apex. At low angles of incidence the region of high RMS can be seen to begin to split into two. The 'primary' region (1) extends from the apex to the trailing edge whereas the 'secondary' region (2), which forms as incidence is increased, is seen as a branch of the primary emanating downstream of the apex and terminating short of the trailing edge.

Figure 5 shows the RMS pressure distribution across the span of the wing at two chord stations (x/c = 0.2 and 0.3875) at an incidence of 14°. Also plotted is the corresponding mean negative C_P distribution. It is clear from both plots that the primary region of high RMS pressure lies inboard of the centreline of the primary vortex core. The secondary RMS pressure region, when apparent, lies outboard of the core. These plots are typical of the RMS pressure distribution over the incidence range corresponding to post-vortex formation and pre-vortex breakdown. The presence of a high RMS pressure region inboard of the vortex core was also observed by Woods and Wood [27] in their work on novel planforms.

A series of contour plots of the RMS pressure distribution on the leeward surface of the wing for four angles of incidence (14°, 16°, 18° and 20°) are shown in Figure 6. At 14° incidence, it can be seen that the secondary branch of high RMS pressure first shown in Figure 4 is still apparent (1) although it has begun to fragment. More significantly, an additional peak of high RMS pressure is forming on the ridge of the primary region at a point close to the trailing edge (2). Careful scrutiny of all contour

plots revealed that this additional peak first appeared at this location on the wing at an incidence of 11° (not shown). The significant features accompanying the appearance of the additional peak are a 'waisting' of the above-described ridge upstream of the peak centre (3) followed by a significant expansion towards the peak. The narrowest part of the waist corresponds to the minimum in a small localised trough of RMS pressure which occurs before the rapid increase towards the peak. As the incidence increases further, the additional peak of high RMS pressure expands in all directions and the waist moves upstream. At 18° and 20° it is possible to detect the beginning of the upstream movement of the centre of the peak but this occurs much more slowly than either the expansion of the high RMS pressure peak or the movement of the waist.

3.3 Analysis Of The Power Spectrum Of Pressure Fluctuations

Previous work by Gursul [25] has identified a dominant frequency in the coherent pressure fluctuations observed on delta wings downstream of vortex breakdown. It was thought that this frequency is associated with the helical mode instability of the vortex breakdown flow field. It has also been shown by Mabey [26] that this frequency is more or less a constant for a given geometry and angle of attack. A frequency analysis was performed as part of the present study. The power spectrum of the sampled pressure data at each angle of incidence was calculated for 42 pressure transducers. The transducers chosen were those identified by the earlier analyses as being located under the path of the vortex core centreline and in the region of high RMS pressure inboard of the vortex core.

A series of power spectra for the transducer located at x/c = 0.55, y/s = 0.6 at four angles of incidence (14°, 16°, 18° and 20°) are shown in Figure 7. At an incidence of 14°, there is a very low frequency component of around 5Hz which dominates the spectrum. The exact nature and cause of this component is as yet unclear. It is noted that this phenomenon has not been described elsewhere and the results of the visualisation tests in the present study do not permit any detailed conclusions to be drawn. However, it first appears in the spectrum of each analysed transducer at an incidence of 2°, which coincides with the first appearance of the ridge of high

negative C_P in the pressure data. Further analysis reveals three spatial and temporal trends. Firstly, regarding the behaviour of the magnitude and bandwidth of the low frequency component. They both increase towards the apex of the wing. Secondly, they are at a maximum underneath and immediately inboard of the path of the vortex core and decrease dramatically towards the wing centreline. Thirdly, they appear to be independent of incidence between post-vortex-formation and pre-vortex breakdown.

At 16° incidence, the magnitude of the low frequency component, which has remained roughly constant since its first appearance, has dropped to about half of its value at 14° incidence. In addition, another band of higher frequencies centred around 220Hz can be seen; these first appear at 15°. This behaviour is typical of the transducers analysed, although the sudden drop in magnitude of the low frequency component occurs at a higher incidence towards the apex of the wing. Similarly, the higher frequency band appears later closer to the apex. Note that whatever the chordwise location, the initial appearance of the higher frequency signals always occurs before the fall in magnitude of the low frequency component. In agreement with previous work [25], the centre of the higher frequency band was found to occur at a higher frequency towards the apex of the wing. For all chordwise locations an increase in incidence tends to decrease the central frequency of the high frequency band while the strength and bandwidth increase.

In the work by Mabey [26] it was shown that the non-dimensional frequency parameter of the quasi-periodic excitation caused by vortex bursting is constant over a given incidence range. This incidence range is characterised by the presence of vortex breakdown in a region between the trailing edge and the apex of the wing. The limits of this region are far enough from either the apex or the trailing edge so as to be unaffected by their non-linear characteristics. It was suggested that this constant has a value of about 0.4 for delta wings of a sweep angle of 60°. Figure 8 shows four plots of excitation frequency, grouped by spanwise position, against chordwise location at different angles of incidence (α = 14°, 16°, 18° and 20°). Also plotted are lines of constant n from n = 0.1 to 0.6 (after Woods and Wood [27]). The four plots show that the excitation frequencies observed in this work, which take into account the path of

the vortex core as well as the high RMS region inboard of the core, are in close agreement with Mabey's observations [ibid.]. Careful examination of the data in these plots reveals a tendency for slightly higher excitation frequencies in the high RMS pressure region inboard of the vortex core at a given chordwise position and incidence. However, the data for this 60° delta wing do not reveal the much higher excitation frequencies that have been observed previously by Woods & Wood [ibid.] in the high RMS pressure region of a more complex wing planform.

Mabey [ibid.] has also suggested that a unique frequency parameter can be found for all delta wings which takes into account the sweep angle as well as the angle of incidence. It was suggested that the value of this modified frequency parameter n_m is 0.25 ± 0.02. Figure 9 shows three plots of modified frequency parameter against incidence for four chord positions (x/c = 0.3875, 0.55, 0.65 and 0.8). Again, the data measured over the majority of the planform show a close agreement with Mabey's previous work.

3.4 Visualisation

Previous work by Lowson [4] has shown that, unlike the position of vortex breakdown, the position of the main vortex core is significantly affected by Reynolds number. Lowson displayed results from a number of tests involving delta wings tested in both air and water. The results were plotted as non-dimensional spanwise position against the ratio of incidence to semi-apex angle. It is clear from Lowson's results that the lateral position of the vortex core at a given ratio of incidence to semi-apex angle was further outboard for those tests in air at high Reynolds numbers, compared with those at low Reynolds numbers in air or water. Similarly, the vertical position of the vortex core for tests at high Reynolds numbers is closer to the surface of the wing than at lower Reynolds numbers although the effect is not so marked. It was suggested that the smaller turbulent secondary vortex structure which forms at high Reynolds numbers in air is not as effective in displacing the primary vortex as its larger laminar counterpart which exists at lower Reynolds numbers in both air and water. In this respect, the results from the visualisation tests done as part of the present study show agreement with Lowson's findings. At a Reynolds number of 10000 and at an

incidence of 10°, the lateral position of the vortex core was found to oscillate very gently about a mean position of y/s = 0.5 compared with the findings of the pressure data at a Reynolds number of 2.7 x 10^6 which place the centre of the vortex at y/s = 0.7. There were slight variations in lateral core position at different chordwise locations but these did not follow any particular pattern. It is thought that the unusual shape of the windward surface of the wing may have an effect on vortex core position but this has not been positively determined. For all chordwise stations the position of the vortex core moved outboard as incidence was increased, again this is in agreement with Lowson's findings.

Vortex breakdown was first observed on the wing at x/c = 0.95 at an incidence of 10°. It was seen to progress steadily up the wing until the observations were concluded at an incidence of 20°, when the breakdown position had reached x/c = 0.25. The observed chordwise progression of vortex breakdown is presented in Figure 10. Also plotted on the same axes, is the variation with incidence of the chordwise location of the apex of the expanded region of high RMS pressure which, as shown in Figure 6, is located just aft of the waist. Similarly, the main features identified in the frequency spectra, previously described in section 3.3, are also plotted for the signals from transducers located in the high RMS pressure region at y/s = 0.6. Shown are the chordwise positions of the first appearance of the excitation frequency, the chordwise position of the sudden drop in the low frequency component and the chordwise location at which the excitation frequency becomes dominant.

4.0 DISCUSSION

The results of the mean C_P data analysis have been successful in determining the position of the primary vortex core and its growth as the wing is pitched through a range of incidences. It is however, very difficult to pick out the other significant features of the flow structure. For the 60° wing tested in this study, the presence of the secondary vortex is not discernible. This observation is supported by the smoke tunnel visualisation tests which revealed a small rotational component of velocity in the secondary vortex structure throughout the incidence range tested. It is also not possible to detect the arrival of vortex breakdown over the trailing edge of the wing. The major problem with the mean C_P data is the broadening and reduction in magnitude of the suction peak over the length of the vortex due to the conical nature of the flow structure [31].

Previous work [12] which used velocity measurements to determine vorticity variations, has identified a region of high turbulent kinetic energy ($0.5\ q^2/U^2$) on the surface of the wing inboard of the primary vortex core but outboard of the primary attachment zone. Similarly, two smaller regions of similar energy intensity have also been identified just above the surface of the wing, and these are located in areas which possibly correspond to the separation and reattachment zones of the secondary vortex. In the light of this, it is thought that the primary region of high RMS pressures, (an indication of the amplitude of the pressure fluctuations) observed inboard of the vortex core (Figure 4, location (1)) is associated with a region of localised but highly turbulent flow within the feeding vortex sheet between the vortex core and the primary attachment region. Similarly, it is thought that the secondary region of high RMS pressures observed outboard of the vortex core (Figure 4, location (2)) is somehow associated with the formation of the secondary vortex structure.

It is clear from Figure 10 that the first appearance of the excitation frequency occurs ahead of the breakdown point shown by the visualisation data. The first appearance of the higher frequency component shows very good agreement with the waisting of the high RMS pressure contours shown in Figure 6, location (3). It is likely that the appearance of the excitation frequency, the waisting of the RMS pressure contours and

the associated localised trough of RMS pressure magnitude (described in section 3.2) are indicative of the first subinterval of the breakdown region first described by Leibovich [32]. This subinterval is characterised by an axial deceleration of the approach flow and the formation of a stagnation point on the vortex axis. It is also possible that the above observations may be associated with an increase in the 'helix angle' of the vortex core velocity [33] during the deceleration phase. A change in the flow direction from that with a greater chordwise component to that with a predominantly spanwise component would align the flow more towards the surface normal direction at the primary reattachment point. It is suggested that this would tend to increase the frequency of pressure fluctuations, as any two pressure disturbances travelling at a similar velocity would cover a shorter distance in the same time-frame. Similarly, the 'sharpening' of the angle of reattachment would tend to reduce the RMS pressure 'footprint' immediately inboard of the reattachment point both in terms of magnitude and width.

Figure 10 also indicates the incidence of the sudden drop in the magnitude of the low frequency component of the frequency spectra. The similarity in behaviour between this and the visualisation data away from the apex and trailing edge, and especially with the RMS pressure data would indicate that this phenomenon is associated with the point of vortex breakdown. The cause of this low frequency component needs explanation. It could be associated with a very low frequency oscillation of the main vortex core during the post-vortex formation/pre-vortex breakdown phase. It is suggested that this oscillation is caused by the cyclic expansion and contraction of the secondary vortex structure. The secondary vortex structure displaces the primary vortex inboard as it grows and allows reinstatement of the primary vortex position as it contracts. This phenomenon has been recorded previously by a number of researchers, particularly Gad-el-Hak & Blackwelder [3], Payne et al [26] and Lee & Ho [34] and was observed in the visualisation tests described in section 3.4. At the breakdown point of the primary vortex which immediately follows that of the secondary vortex [6], the low frequency component associated with the formation and dissolution of the secondary vortex structure suddenly reduces in magnitude and the higher frequency component associated with the burst primary vortex becomes progressively stronger. As shown in Figure 10 however, a delay exists before the

higher frequency component becomes dominant. This apparently occurs after breakdown and as such may be associated with the fully broken down state. Once breakdown has fully developed, the magnitude of the low frequency element drops considerably and the dominance of the higher excitation frequency ensues.

Figure 10 indicates a similarity in behaviour of the vortex breakdown position determined by the smoke visualisation data and that obtained from the RMS pressure data analysis. Discrepancies do occur very close to the apex of the wing and the trailing edge, the former due mainly to the poor pressure transducer density in this area compared with further down the wing (see Figure 1) and the latter due to the difficulties in pin-pointing the exact breakdown position so close to the trailing edge during the visualisation tests. It would appear that the arrival of vortex breakdown at the trailing edge of the wing and subsequently at chord stations upstream heralds a substantial increase in turbulent kinetic energy in this region which may be associated with the generation of a negative azimuthal component of vorticity. This was previously shown by Brown & Lopez [33] to be necessary for the axial component of velocity in the vortex core to be brought to rest and for vortex breakdown to take place. Brown & Lopez have shown that the development of negative azimuthal vorticity on a diverging stream surface that bounds the vortex core will induce a negative axial velocity on the vortex axis which, by continuity, will lead to a further divergence of the stream surface and a further increase in negative vorticity. It is suggested that it is this mechanism that is associated with the rapid increase in magnitude of the high RMS pressure region downstream of breakdown as well as the broadening of the region across the wing in a spanwise direction (Fig. 6, location (2)) as the wing incidence is increased.

5.0 CONCLUSIONS

Detailed experiments have been carried out on a 60° delta wing with sharp leading-edges. The instantaneous pressure distribution on one half of the leeward surface of the wing has been successfully measured over a range of incidence using a large number of closely spaced pressure transducers coupled to an advanced data acquisition system capable of sampling at a high rate. The advantages of high spatial and temporal resolution pressure measurements lie in the ability to obtain high quality statistical data of the pressure fluctuations over the whole surface of the wing. A number of observations have been made regarding the RMS pressure distribution and the power spectra of the pressure fluctuations which have been supported by the results from smoke visualisation tests. It is suggested that the deceleration and eventual stagnation of the axial velocity within the vortex core, which acts as a pre-cursor to vortex breakdown, is indicated by a 'waisting' of the contours in the region of high RMS pressure inboard of the vortex core. Similarly, it is suggested that the onset of the fully broken down state is indicated by an expansion of the same RMS pressure contours immediately downstream of the waist and is accompanied by a characteristic change in the frequency signature of the pressure fluctuations.

The work presented in this study has demonstrated the potential to investigate breakdown using pressure measurements. The high temporal resolution of the current data acquisition system provides the scope to extend the RMS pressure analysis to pitch up/down and oscillatory cases. This work is currently in progress and will, in the near future, be supplemented by detailed flow-field surveys carried out at the same Reynolds numbers as the pressure measurement tests.

ACKNOWLEDGEMENTS

The wind tunnel tests reported in this study were carried out with funding from the Engineering and Physical Sciences Research Council (EPSRC), GKN Westland Helicopters Ltd., the Defence Evaluation & Research Agency (DERA) and Glasgow University under contract GR/H48330. The authors also wish to acknowledge the additional support of the EPSRC through RS Quota award 96300150 and the support provided for the flow visualisation activities by the Nuffield Foundation. Finally, the authors are indebted to Prof. R. Galbraith of the Department of Aerospace Engineering for his continual support and encouragement throughout this project.

REFERENCES

1. Lambourne, N. C. and D. W. Bryer. The bursting of leading-edge vortices - some observations & discussion of the phenomenon. *R & M, No. 3282, Aeronautical. Research. Council.* 1961.
2. Elle, B. J. On the breakdown at high incidences of the leading-edge votices on delta wings. *J. Royal Aeronautical Soc.* 1960. **64**. (April): 491-493.
3. Gad-el-Hak, M. and R. F. Blackwelder. Control of the discrete vortices from a delta wing. *AIAA J.* 1987. **25**. (8): 1042-1049.
4. Lowson, M. V. Visualisation measurements of vortex flows. *J. Aircr.* 1991 **28**. (5): 320-327.
5. Payne, F. M., T. T. Ng, et al. Visualisation & flow surveys of the leading-edge vortex structure on delta wing planforms. *AIAA Paper No. 86-0330.* 1986.
6. Atta, R. and D. Rockwell. Hysteresis of vortex development and breakdown on an oscillating delta wing. *AIAA J.* 1987. **25**. (11): 1512-1513.
7. den Boer, R. G. and A. M. Cunningham Jr. Low-speed unsteady aerodynamics of a pitching straked wing at high incidence - Part 1 : Test program. *J. Aircr.* 1990. **27**. (1): 23-30.
8. Gad-el-Hak, M. and C.-M. Ho. The pitching delta wing. *AIAA J.* 1985. **23**. (11) 1660-1665.
9. Gad-el-Hak, M. and C.-M. Ho. Unsteady vortical flow around three-dimensional lifting surfaces. *AIAA J.* 1986. **24**. (5): 713-721.
10. LeMay, S. P., S. M. Batill, et al. Vortex dynamics on a pitching delta wing. *J. Aircr.* 1990. **27**. (2): 131-138.
11. Wolffelt, K. W. Investigation on the movement of vortex burst position with dynamically changing AoA for a schematic deltawing in a water tunnel with correlation to similar studies in a windtunnel. AGARD CPP 413, 1986.
12. Honkan A. and J. Andreopoulous. Instantaneous three-dimensional vorticity measurements in vortical flow over a delta wing. *AIAA J.* 1997. **35**. (10):1612-1620.
13. Visser, K. D. and R. C. Nelson (1993). "Measurements of circulation & vorticity in the leading edge vortex of a delta wing." *AIAA J.* 1993. **31**. (1): 104-111.

14. Cornelius, K. C. Analysis of vortex bursting utilising three-dimensional Laser measurements. *J. Aircr.* 1995. **32**. (2): 297-306.
15. Miau, J. J., R. C. Chang, et al. Non-uniform motion of leading-edge vortex breakdown on ramp-pitching delta wings. *AIAA J.* 1992. **30**. (7): 1691-1702.
16. Payne, F. M., T. T. Ng, et al. Experimental study of the velocity field on a delta wing. *AIAA Paper No. 87-1231*. 1987.
17. Cipolla, K. M. and D. Rockwell. Flow structure on a stalled delta wing subjected to small amplitude pitching oscillations. *AIAA J.* 1995. **33**. (7): 1256-1262.
18. Lin, J.-C. and D. Rockwell. Transient structure of vortex breakdown on a delta wing. *AIAA J.* 1995. **33**. (1): 6-12.
19. Magness, C., O. Robinson, et al. Unsteady crossflow on a deltawing using Particle Image Velocimetry. *J. Aircr.* 1992. **29**. (4): 707-709.
20. Gursul, I. and H. Yang. Vortex breakdown over a pitching delta wing. *J. Fluids & Structures*. 1995. (9): 571-583.
21. Rediniotis, O. K., H. Stapountzis, et al. Vortex shedding over delta wings. *AIAA J.* 1990. **28**. (5): 944-946.
22. Thompson, S. A., S. M. Batill, et al. (1990). Delta wing surface pressures for high angle of attack manoeuvres. *AIAA Paper No. 90-2813* 1990.
23. Vaughan, J. P. and N. J. Wood. Pressure measurements on a half delta wing oscillating in pitch. *Aero. J.* 1995. **99**. (990): 432-438.
24. Greenwell, D. I. and N. J. Wood. Determination of vortex burst location on delta wings from surface pressure measurements. *AIAA J.* 1992. **30**. (11) 2736-2739.
25. Gursul, I. Unsteady flow phenomena over delta wings at high angle of attack. *AIAA J.* 1994. **32**. (2): 225-231.
26. Mabey, D. G. Unsteady vortex flow phenomena on delta wings at high angles of incidence. *20th Congress of the International Council of the Aeronautical Sciences, Sorrento, Italy*. 1996.
27. Woods, M. I. and N. J. Wood. Unsteady aerodynamic phenomena on novel wing planforms. *20th Congress of the International Council of the Aeronautical Sciences, Sorrento, Italy*. 1996.
28. Parker, A. G. (1976). Aerodynamic characteristics of slender wings with sharp leading edges - A review. *J. Aircr.* 1976. **13**. (3): 161-168.

29. Jarrah, M. A. M. Visualisation of the flow about a delta wing manoeuvring in pitch to very high angle of attack. *ASME Publication FED*, 1990. **92**: 109-116.
30. Thompson, S. A., S. M. Batill, et al. Separated flowfield on a slender wing undergoing transient pitching motions. *AIAA J.* 1991. **28**. (8): 489-495.
31. Hall, M. G. A theory for the core of a leading-edge vortex. *J. Fluid Mech.* 1961. **11**: 209-228.
32. Leibovich, S. The structure of vortex breakdown. *Ann. Rev. Fluid Mech.* 1978. **10**: 221-246.
33. Brown, G. L. and J. M. Lopez. Axisymmetric vortex breakdown, Part 2 - Physical mechanisms. *J. Fluid Mech.* 1990. **221**: 553-576.
34. Lee, M. and C.-M. Ho. Lift force of delta wings. *Applied. Mech. Rev.* 1990. **43**. (9): 209-221.

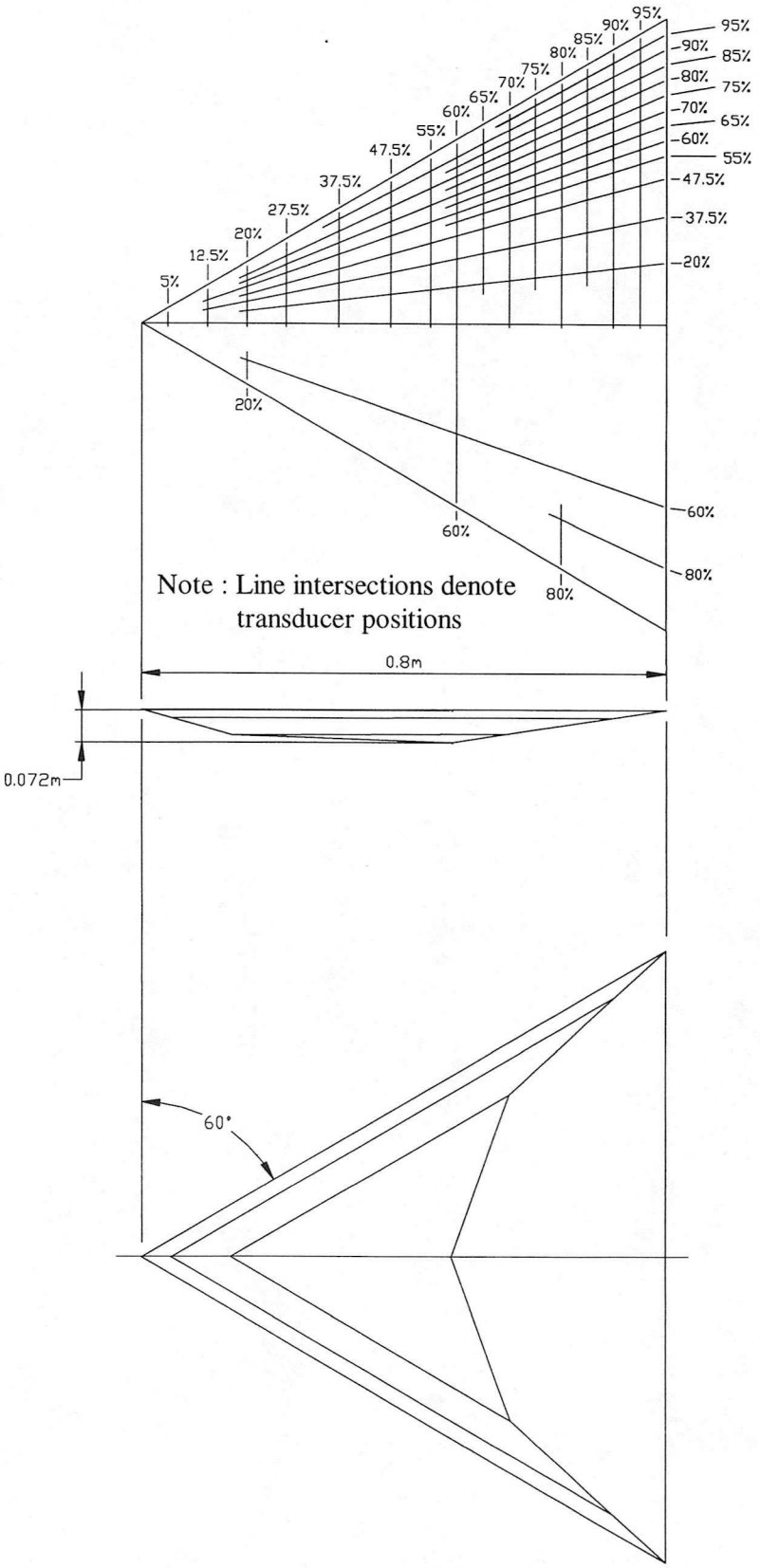

Figure 1 - The delta wing model leeward surface transducer positions & windward surface shape

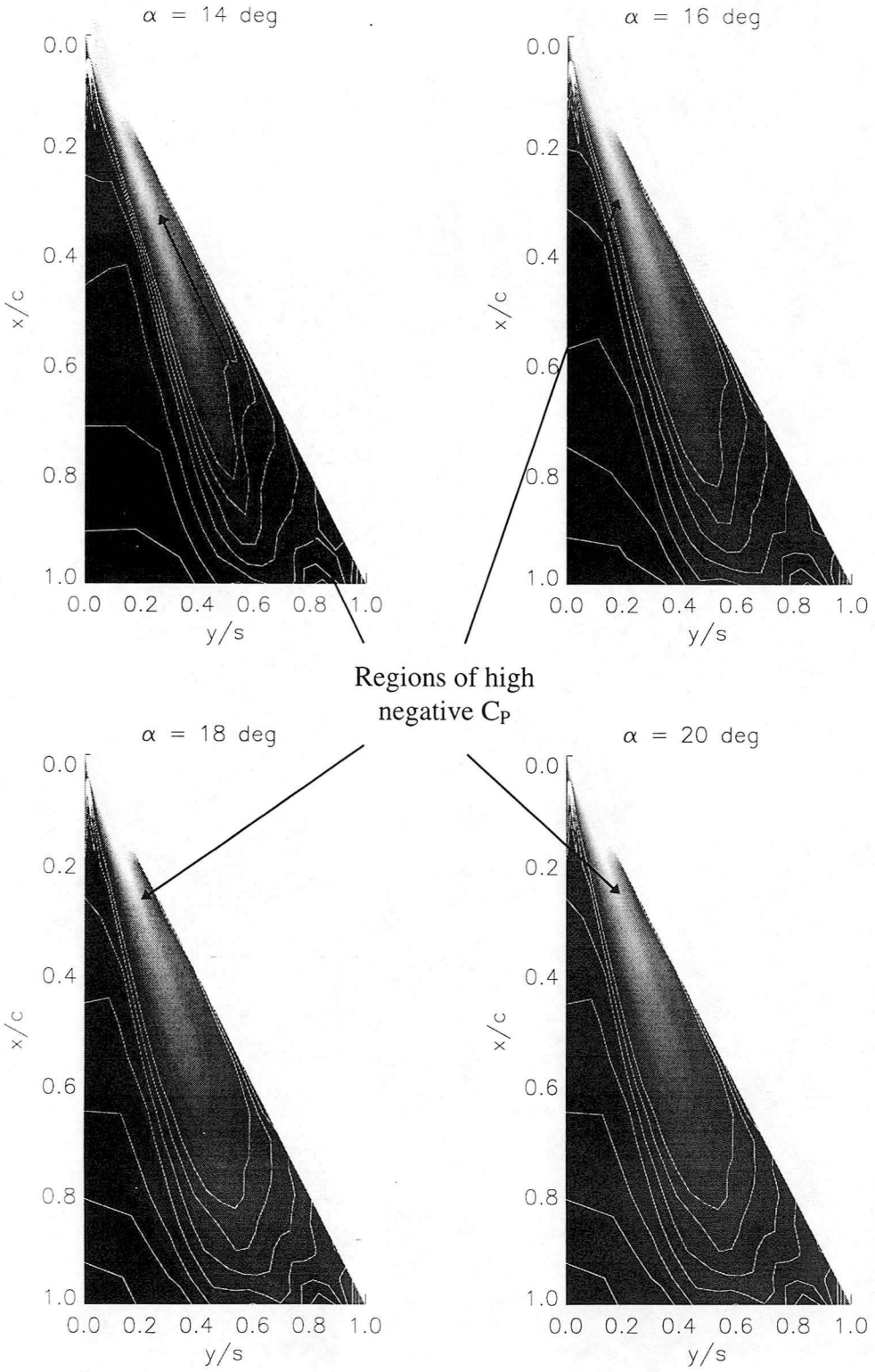

Figure 2 - Contours of mean negative C_P at four angles of incidence

($\alpha = 14°$, $\alpha = 16°$, $\alpha = 18°$ and $\alpha = 20°$)

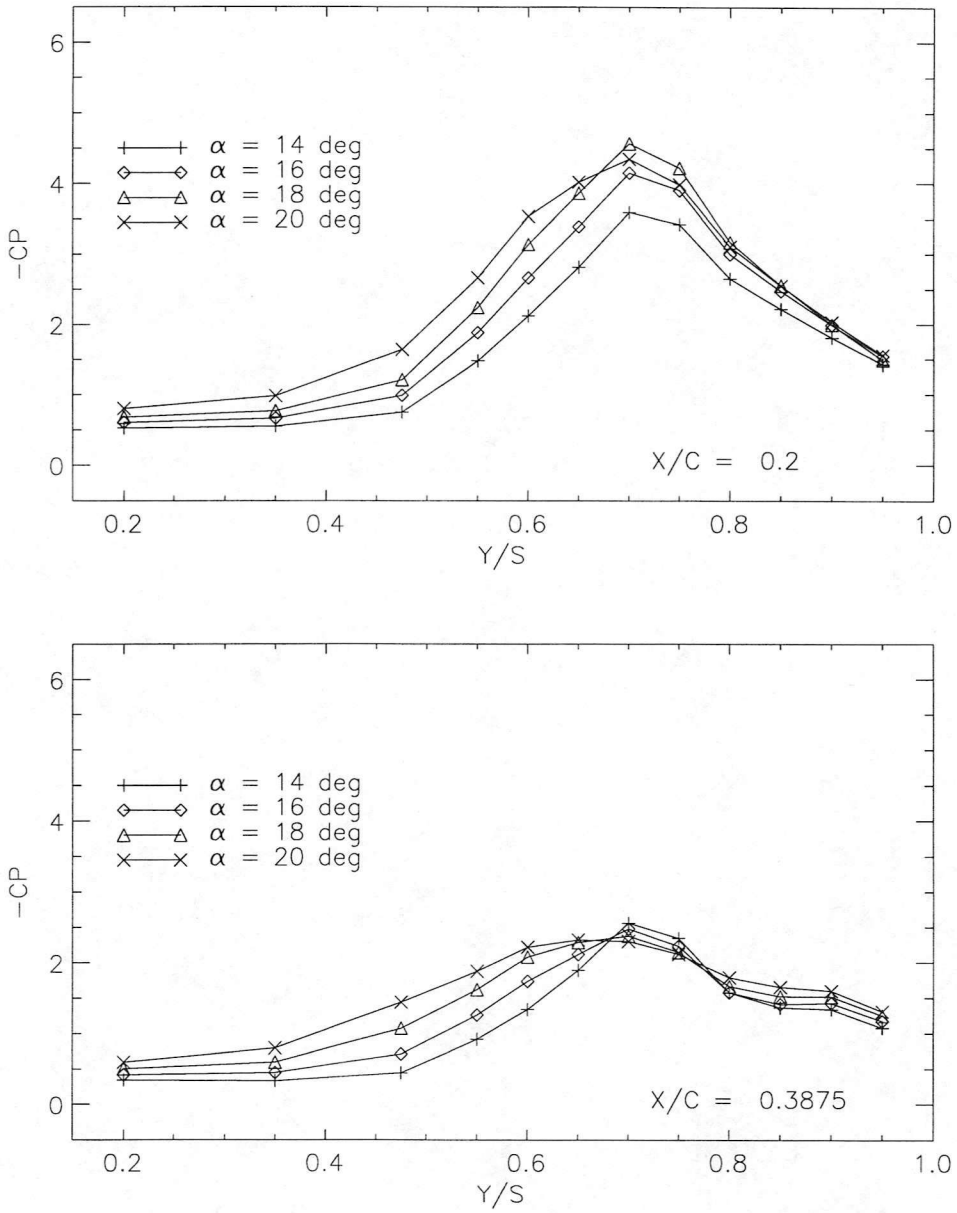

Figure 3 - Plots of $-C_P$ against non-dimensional spanwise position

at four angles of incidence for each of two chordwise positions

($\alpha = 14°$, $\alpha = 16°$, $\alpha = 18°$ and $\alpha = 20°$)

(x/c = 0.2 and x/c = 0.3875)

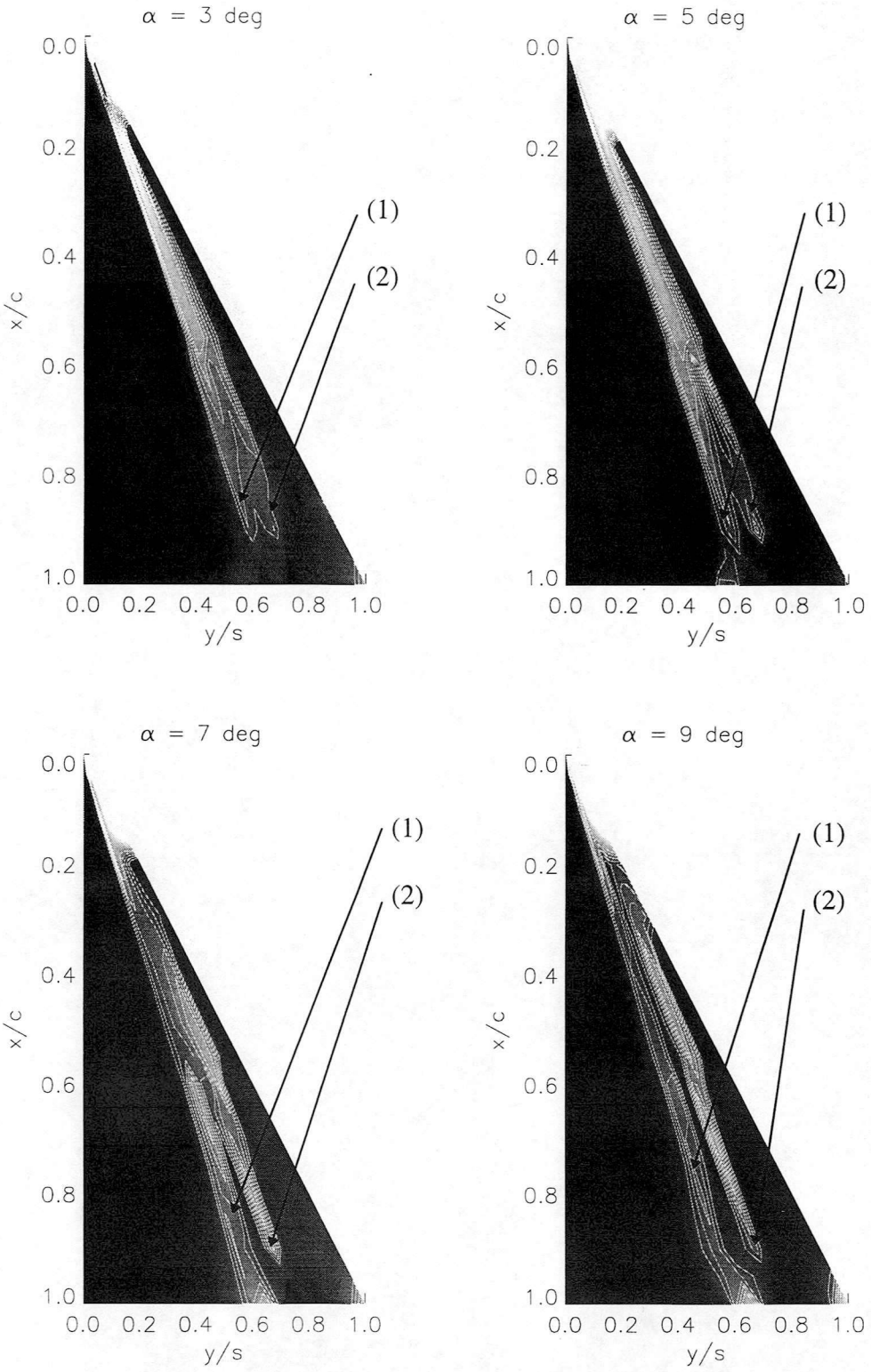

Figure 4 - Contours of RMS surface pressure at four angles of incidence

($\alpha = 3°$, $\alpha = 5°$, $\alpha = 7°$ and $\alpha = 9°$)

(1) Primary region of high RMS Pressure

(2) Secondary region of High RMS pressure

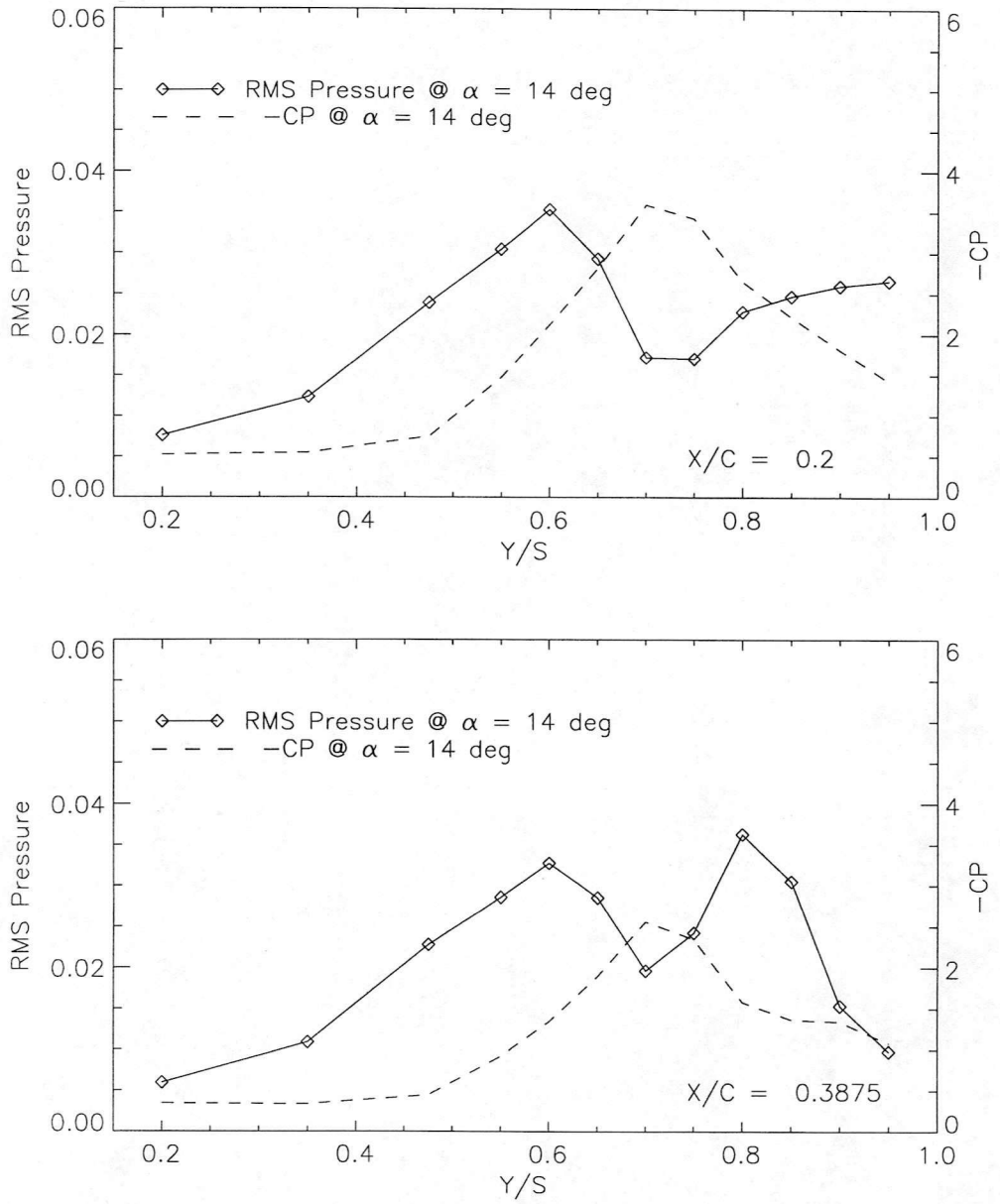

Figure 5 - Comparison of the spanwise distribution of mean negative C_P and RMS pressure at an incidence of 14° for two chordwise positions (x/c = 0.2 and x/c = 0.3875)

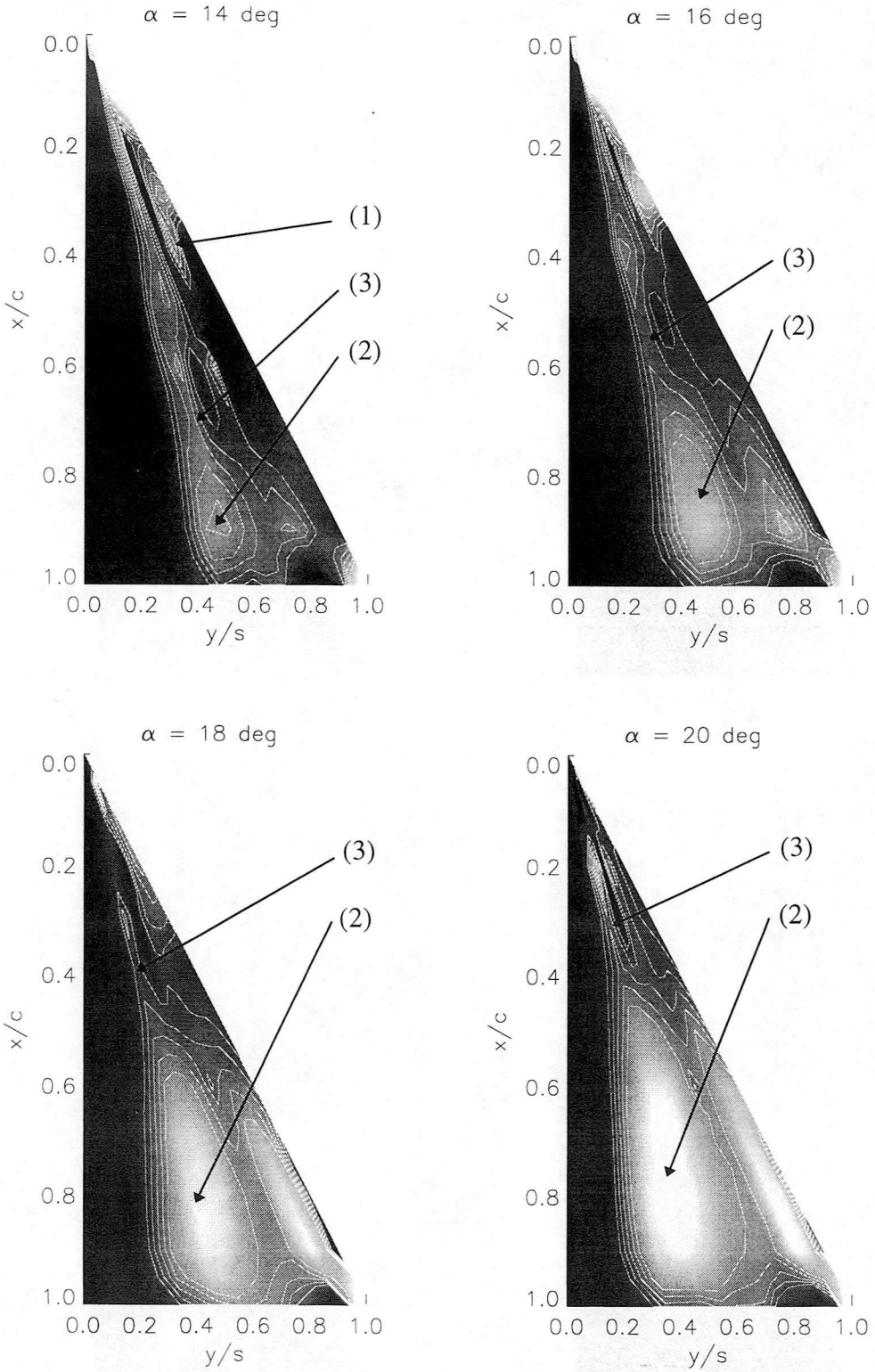

Figure 6 - Contours of RMS surface pressure at $\alpha = 14°, 16°, 18°$ and $20°$

Key : - (1) Secondary region of high RMS pressure

(2) Additional peak of high RMS pressure

(3) 'Waisting' of RMS pressure contours

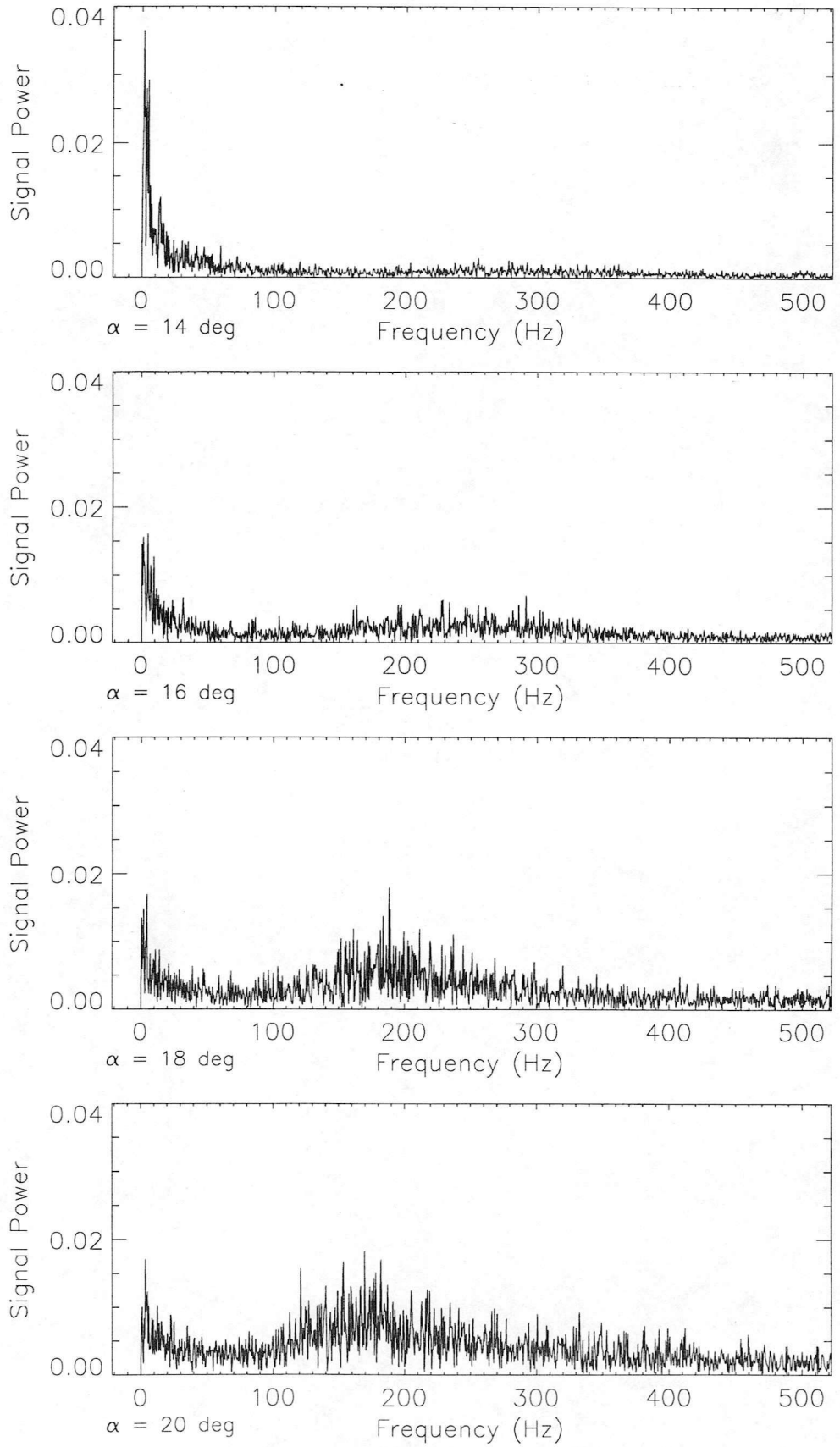

Figure 7 - Power spectrum of pressure data at four angles of incidence for transducer 38, located at x/c = 0.55, y/s = 0.6

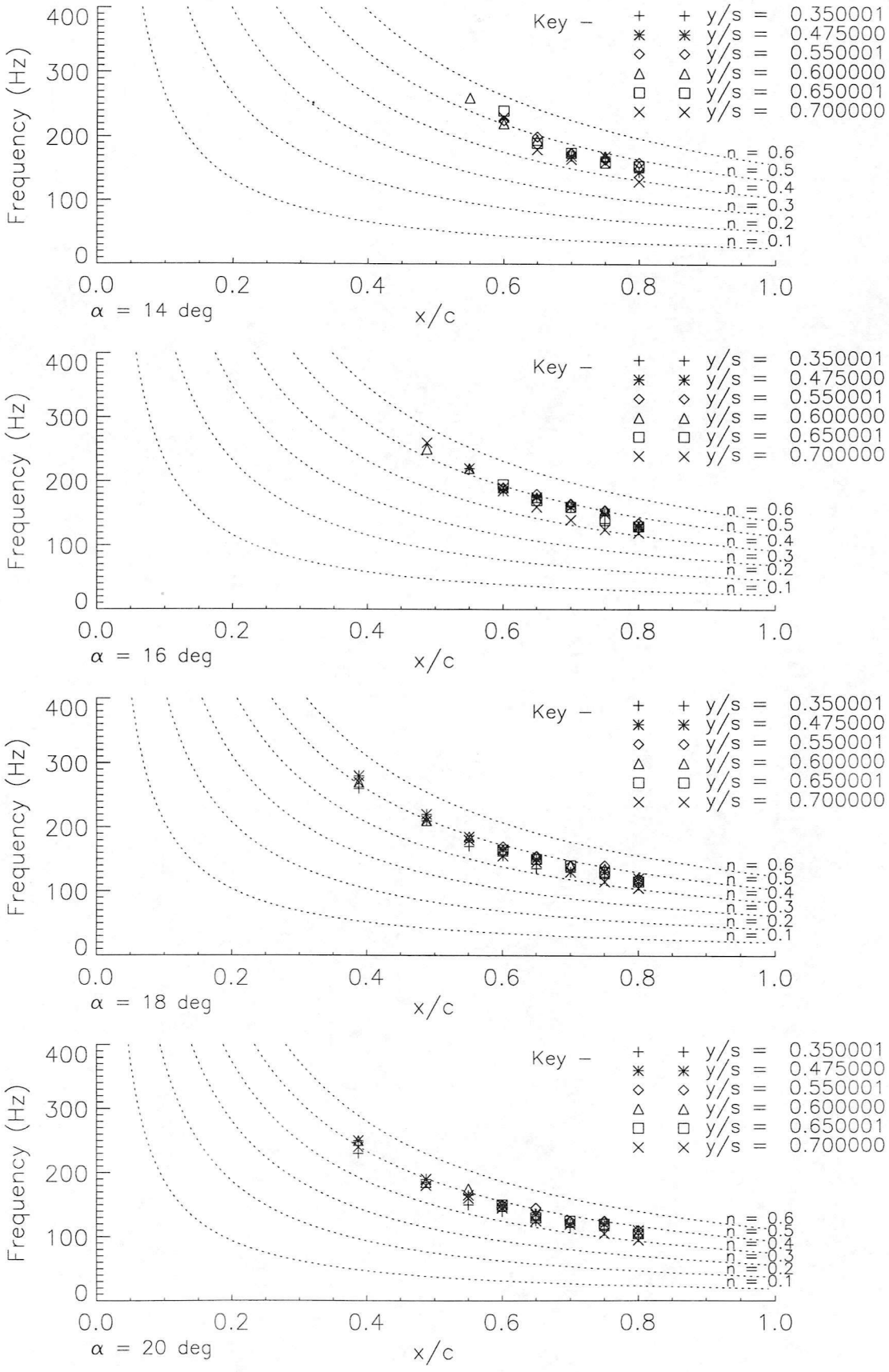

Figure 8 - Plot of the central frequency in the excitation frequency band against chordwise position at four angles of incidence (α = 14°, 16°, 18° and 20°), showing only the transducers where the excitation frequency was apparent. Transducers grouped by spanwise location. Also plotted are six values of constant non-dimensional frequency parameter n.

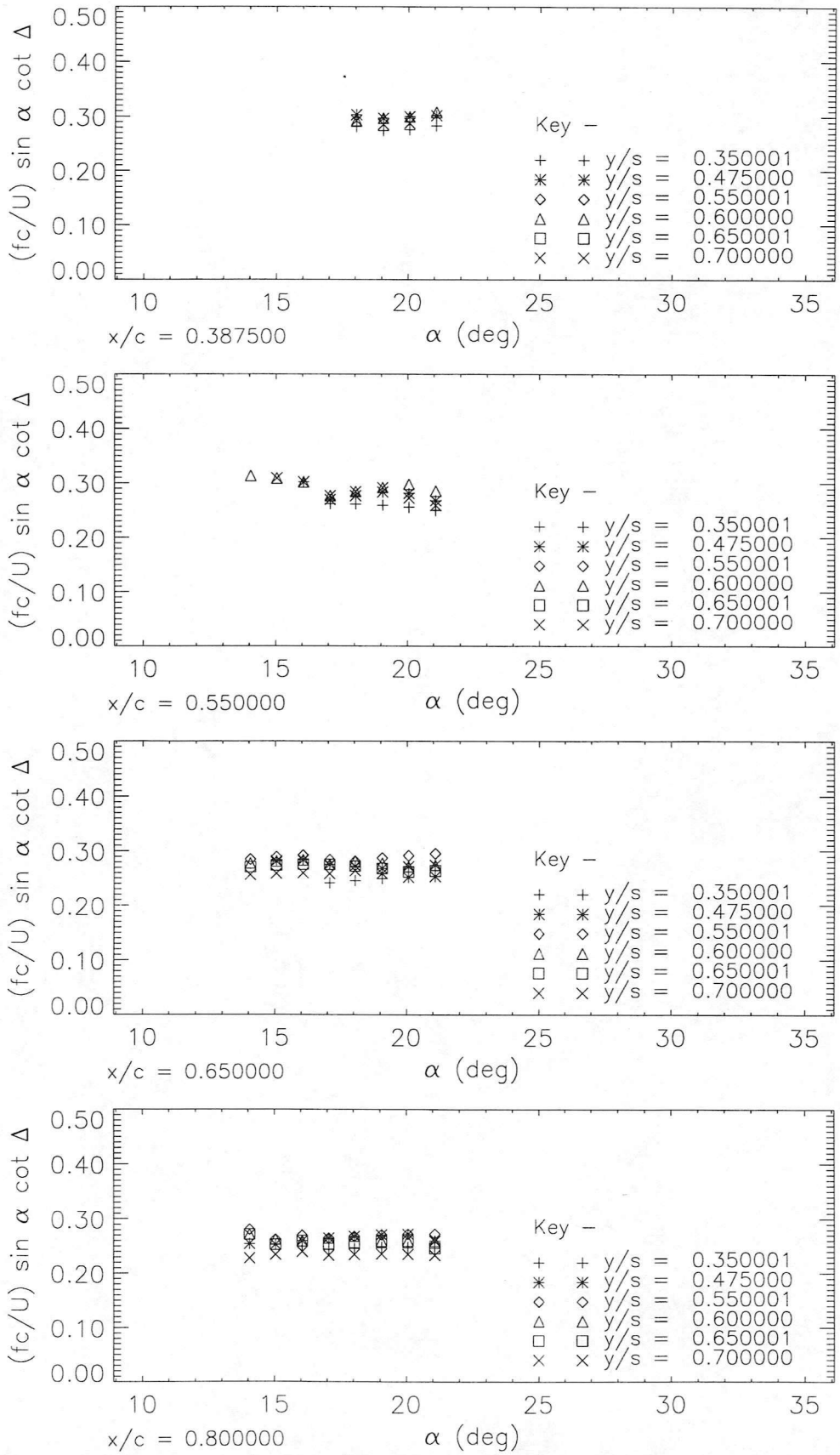

Figure 9 - Plot of modified non-dimensional frequency parameter n_m against angle of incidence at four chordwise locations (x/c = 0.3875, 0.55, 0.65 and 0.8) showing only the transducers where the excitation frequency was apparent. Transducers grouped by spanwise location. (After Mabey [**]).

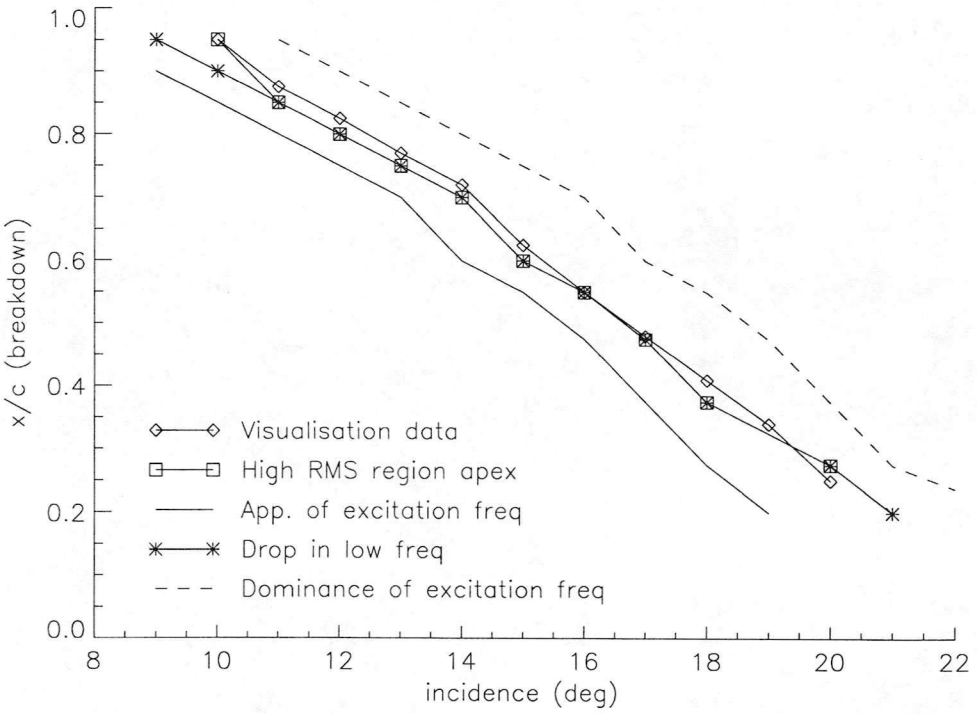

Figure 10 - Plot of $x/c_{(breakdown)}$ against incidence showing :

1. Results of smoke flow visualisation tests.

2. The apex of the region of high RMS pressure (Figure 6, location 2).

3. The first appearance in the power spectrum of the high frequency component.

4. The sudden drop in magnitude of the low frequency component.

5. The eventual domination of the spectrum by the high frequency component.